IOP Conf. Series: Materials Science and Engineering **192** (2017) 012017 doi:10.1088/1757-899X/192/1/012017

On the theory of self-similar phase transitions with a mushy layer

D V Alexandrov, I V Alexandrova and A A Ivanov

Department of Theoretical and Mathematical Physics, Laboratory of Multi-Scale Mathematical Modeling, Ural Federal University, Ekaterinburg, 620000, Russian Federation

E-mail: dmitri.alexandrov@urfu.ru

Abstract. It is well-known that directional crystallization processes frequently occur in unsteady-state manner. One of such time-dependent crystallization regimes is the self-similar process characterizing by the scaled combination $\xi/\sqrt{t}$ between the spatial coordinate ξ (directed along the solidification axis) and time t. Such scaling relation usually establishes when the crystallization process is far from its initial stage $t = 0$. In this paper, we consider some approximate heuristic relations describing the self-similar solidification mode.

1. Introduction

A mathematical description of directional crystallization plays a very important role in different applications such as the crystal growth, engineering, geophysical and metallurgical process [1–9]. So, for example, the mathematical models allow to predict many properties of solids produced by solidification. When the liquid is a melt (a mixture of two or more components) its solidification process completely differs from solidification of pure liquid. In particular, various distributions of impurity in the solid phase leads to different mechanical and physical properties of ingots. This phenomenon arises due to the impurity displacement into the liquid phase by the moving solidification front. When the impurity displacement is rather large, the constitutional supercooling originates ahead of the planar solid-liquid interface [10] and, generally speaking, the two-phase zone (mushy layer) appears. Moreover, the solid nuclei in the form of newly born crystals may evolve in this layer. The authors of references [11–13] developed a full set of thermodynamic equations for a mushy zone and solved a mush-reduced set of them approximately for the constrained growth of a binary alloy. A more complete solution has since been given in references [14–18] for the transient and steady-state solidification conditions.

Note that the constitutional supercooling origination (this occurs if the concentration gradient $G_C = m\partial C_L/\partial\xi$ exceeds the temperature one $G = \partial\theta_L/\partial\xi$ at the planar front; here m is the liquidus slope determined from the phase diagram, C_L and θ_L are the concentration and temperature fields in the liquid phase) leads under certain circumstances to the mushy zone solidification and the classical description of crystallization by means of the planar front model becomes inapplicable. However, if the process is far from a cooled wall and the constitutional supercooling and/or the mushy layer are absent, the solidification process with a planar front (after a lapse of time) approaches to its self-similarity. This solidification scenario was experimentally studied by Huppert and Worster [19] on the basis of aqueous solution of sodium nitrate. At first, the solidification process occurs within the framework of the Stefan

thermodiffusion problem with a planar front. Then the planar shape of the solid-liquid interface destroys and the process takes place with a mushy layer (see, for example, Figure 3 in [19]).

2. Self-similar model

Let us consider a unidirectional solidification process of a binary melt or solution directed along the ξ axis. The cooled wall is placed at $\xi = 0$ and regions $0 < \xi < \Sigma(t,\zeta)$ and $\Sigma(t,\zeta) < \xi < \infty$ are filled with the solid and liquid phases, respectively. Before a point of time when the constitutional supercooling originates, the process is described within the framework of the classical thermodiffusion model with a planar front $\Sigma(t)$. Namely, the temperature and concentration fields in both the phases are governed by the following parabolic-type equations

$$\frac{\partial \theta_L}{\partial t} = a_L \Delta \theta_L, \ \frac{\partial C_L}{\partial t} = D_L \Delta C_L, \ \Sigma(t) < \xi < \infty, \tag{1}$$

$$\frac{\partial \theta_S}{\partial t} = a_S \Delta \theta_S, \ \frac{\partial C_S}{\partial t} = D_S \Delta C_S, \ 0 < \xi < \Sigma(t). \tag{2}$$

Here θ_S and C_S are the temperature and concentration in the solid, a_L and a_S are the thermal diffusivities in the liquid and solid phases, D_L and D_S are the diffusion coefficients in these phases, and $\Delta = \partial^2/\partial\xi^2 + \partial^2/\partial\zeta^2$ is the Laplacian. In the case of solidification with a planar front nothing depends on the spatial coordinate ζ directed perpendicular to the crystallization direction. The thermal and mass balance conditions as well as the equality of both temperatures to the phase transition temperature hold true at the front

$$K_S \frac{\partial \theta_S}{\partial \xi} - K_L \frac{\partial \theta_L}{\partial \xi} = L_V \frac{\partial \Sigma}{\partial t}, \ (1-k) C_L \frac{\partial \Sigma}{\partial t} + D_L \frac{\partial C_L}{\partial \xi} - D_S \frac{\partial C_S}{\partial \xi} = 0, \ \xi = \Sigma(t,\zeta), \tag{3}$$

$$\theta_L = \theta_S = \theta_0 + m C_L + \Gamma \theta_0 K, \ \xi = \Sigma(t,\zeta), \tag{4}$$

where K_S and K_L are the thermal conductivities in the solid and liquid phases, L_V is the latent heat parameter, k is the equilibrium partition coefficient, θ_0 is the phase transition temperature of pure system, Γ is the surface tension, and K is the front curvature. Moreover, we assume that the concentration jump at the front is also given, that is,

$$C_S = k C_L, \ \xi = \Sigma(t,\zeta). \tag{5}$$

The temperatures at the cooled wall and far from the front in the liquid phase are fixed

$$\theta_S = \theta_W, \ C_S = C_W = k C_{L\infty}, \ \xi = 0, \tag{6}$$

$$\theta_L \to \theta_{L\infty}, \ C_L \to C_{L\infty}, \ \xi \to \infty. \tag{7}$$

The model (1)-(7) is valid before the constitutional supercooling origination, that is, before the mushy zone initiation [5, 10]. If the mushy zone exists, the process must be described by means of a mushy layer model. Let us discuss below the mushy layer model when the nucleation within the mush is not taken into account. In this case, equations (1) and (2) are valid in regions $\Sigma_L < \xi < \infty$ and $0 < \xi < \Sigma_S$, where Σ_L and Σ_S stand for the mushy layer - liquid phase and solid phase - mushy layer interfaces while the region $\Sigma_S < \xi < \Sigma_L$ is filled with the mushy layer. The heat and mass transfer processes in the mushy region are governed by the following equations

$$\begin{aligned} &\rho_m c_m \frac{\partial \theta_m}{\partial t} = \frac{\partial}{\partial \xi}\left(K_m \frac{\partial \theta_m}{\partial \xi}\right) + L_V \frac{\partial \varphi}{\partial t}, \\ &\frac{\partial}{\partial t}\left((1-\varphi) C_m\right) = \frac{\partial}{\partial \xi}\left(D_m \frac{\partial C_m}{\partial \xi}\right) - k C_m \frac{\partial \varphi}{\partial t}, \ \Sigma_S < \xi < \Sigma_L, \end{aligned} \tag{8}$$

where θ_m and C_m are the temperature and concentration fields in the mush, φ is the bulk fraction of the solid phase, and $\rho_m c_m(\varphi) = \rho_L c_L(1-\varphi) + \rho_S c_S \varphi$, $K_m(\varphi) = K_L(1-\varphi) + K_S\varphi$, $D_m(\varphi) = D_L(1-\varphi) + D_S\varphi$. Here ρ_S and ρ_L are the densities in the solid and liquid phases, c_S and c_L are the thermal capacities in these phases. The two-phase layer is assumed to be in a state of thermodynamic equilibrium. This means that the temperature in both phases is equal to the phase transition temperature connected with the solute concentration. Let us write down the liquidus line equation in a linear form

$$\theta_m = \theta_0 + mC_m,\ \Sigma_S < \xi < \Sigma_L. \tag{9}$$

The set of equations (8) and (9) must be supplemented by the boundary conditions imposed at both interfaces, i.e.

$$\begin{gathered}\varphi = \varphi_*,\ K_S\frac{\partial\theta_S}{\partial\xi} - K_m\frac{\partial\theta_m}{\partial\xi} = L_V(1-\varphi_*)\frac{\partial\Sigma_S}{\partial t},\ C_S = kC_m,\\ (1-k)(1-\varphi_*)C_m\frac{\partial\Sigma_S}{\partial t} + D_m\frac{\partial C_m}{\partial\xi} = 0,\ \theta_m = \theta_S,\ \xi = \Sigma_S,\end{gathered} \tag{10}$$

$$\varphi = 0,\ C_m = C_L,\ D_m\frac{\partial C_m}{\partial\xi} = D_L\frac{\partial C_L}{\partial\xi},\ \theta_m = \theta_L,\ K_m\frac{\partial\theta_m}{\partial\xi} = K_L\frac{\partial\theta_L}{\partial\xi},\ \xi = \Sigma_L. \tag{11}$$

In addition, we assume that the boundary conditions (6), (7) hold true far from the mushy layer.

In the case of self-similar crystallization, the spatial coordinate ξ and time t are connected by the relation $\xi/\sqrt{t}$ while the planar front position Σ as well as the solid phase - mushy layer Σ_S and the mushy layer - liquid phase Σ_L coordinates in accordance with two models above are expressed as $\Sigma = 2\lambda\sqrt{D_L t}$, $\Sigma_S = 2\lambda_S\sqrt{D_L t}$ and $\Sigma_L = 2\lambda_L\sqrt{D_L t}$, where the parabolic growth rate constants λ, λ_S and λ_L must be found from the model solution. Computations carried out by Worster [20] and instability analysis given by Alexandrov [5] show that the mushy zone originates only after the constitutional supercooling initiation whereas the planar front of solidification is always stable to small morphological perturbations. In other words, if the self-similarity establishes, the planar front shape cannot be destroyed by small temperature or mechanical perturbations, that is, the self-similar Stefan thermodiffusion problem is stable. However, when the constitutional supercooling arises (in this case the process must be described by a mushy layer model; not by the planar front model without a mush), the metastable supercooling zone exists ahead of the solid phase interface. Therefore, the solidification process with a planar front without a mushy layer must be described by the model (1)-(7) whereas the solidification process in the presence of constitutional supercooling and, as a consequence, in the presence of a mushy layer, must be described within the framework of the model (6), (7) and (8)-(11).

Figures 1 and 2 demonstrate the parabolic growth rate constants as functions of the temperature $T_1 \equiv mC_{L\infty} - T_W$ for two sets of parameters given in table 1 ($T_{L\infty} = 15^{\circ}$C and $C_{L\infty} = 14$). The solid curves illustrate the numerical solutions found in [20] and the crosses in Figure 2 represent the experimental values found in [19]. As is seen from the figures, there is a point of bifurcation (intersection of the curves) where $\lambda = \lambda_b \approx 0.15$, $T_1 = T_{1b} \approx 2^{\circ}$C (Figure 1) and $\lambda_b \approx 0.15$, $T_{1b} \approx 1.72^{\circ}$C (Figure 2). This point is responsible for the mushy zone incipience (this happens at $\lambda > \lambda_b$ and $T_1 > T_{1b}$). In other words, the solid phase - mushy layer (λ_S) and mushy layer - liquid phase (λ_L) boundaries appear. It is easy to see that the function $\lambda(T_1)$ has a root-like behavior. Therefore, let us use the following approximate heuristic expression

$$\lambda = \lambda_b + \sqrt{A\,(T_1 - T_{1b})}, \tag{12}$$

where A is a constant. The dashed curves in Figures 1 and 2 are plotted in accordance with expression (12). Our calculations show that A is of the order of 0.75 (Figure 1) and 2 (Figure

Table 1. The physical parameters used for calculations [19, 20].

Property	Set a	Set b $NaNO_3 + H_2O$	Units
Thermal conductivity in liquid, K_L	$1.3 \cdot 10^{-3}$	$1.3 \cdot 10^{-3}$	cal /(cm s °C)
Thermal conductivity in solid, K_S	$1.3 \cdot 10^{-3}$	$5.3 \cdot 10^{-3}$	cal /(cm s °C)
Thermal diffusivity in liquid, a_L	$1.3 \cdot 10^{-3}$	$1.3 \cdot 10^{-3}$	cm^2/s
Thermal diffusivity in solid, a_S	$1.3 \cdot 10^{-3}$	$1.2 \cdot 10^{-2}$	cm^2/s
Diffusion coefficient in liquid, D_L	10^{-5}	10^{-5}	cm^2/s
Diffusion coefficient in solid, D_S	10^{-9}	10^{-9}	cm^2/s
Latent heat per unit volume, L_V	80	73.6	cal/sm^3
Liquidus slope, m	-0.4	-0.4	°C
Segregation coefficient, k	0	0	-
Density of liquid, ρ_L	1	1	gr/cm^3
Density of solid, ρ_S	1	0.48	gr/cm^3

2). Some small deviations of the dashed curves from the solid ones occur near the bifurcation point. This is due to the fact that the self-similar mushy layer is not established in this region. In the case of large values of temperature T_1, the expression above is in good agreement with experimental data.

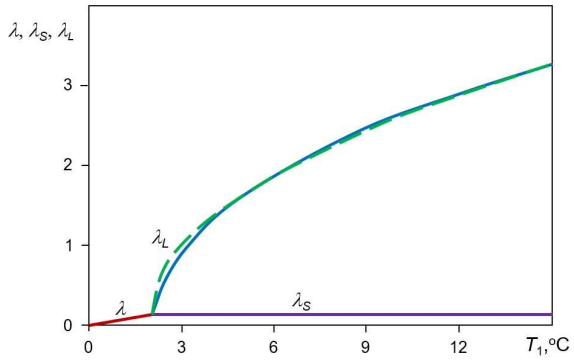

Figure 1. The parabolic growth rate constants for the Set a (table 1).

3. Conclusion

Thus, the main peculiarities of self-similar solidification process seem to be clear. At first, the solidification process occurs in accordance with the classical thermodiffusion model with a planar front. Let us especially emphasize that the velocity of solidification within the framework of this model is a function inversely proportional to the process time, i.e. $d\Sigma/dt = \lambda\sqrt{D_L/t}$. In other words, the front motion is decelerated. This means that the solidification process may occur in accordance with two scenarios. First of them happens if the impurity displacement is slow. If this is really the case, the concentration gradient (G_C) does not exceed the temperature one (G) at the front, and the front shape remains planar. The second possible scenario appears due to the constitutional supercooling origination and, as a consequence, due to the metastable mushy layer initiation. In this case, the solidification scenario must be described by a mushy layer

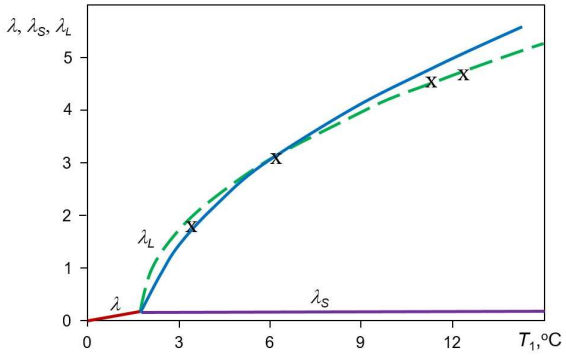

Figure 2. The parabolic growth rate constants for the Set *b* (table 1).

model. What is more, the mushy layer evolution occurs due to the constitutional supercooling so that if it is absent, the self-similar solidification occurs with a planar front.

The theory of unsteady-state solidification with a mushy layer should be extended to take into account the processes of nucleation and growth of newly born crystals in a metastable layer. This can be done on the basis of recently developed theories of transient nucleation for single-component and binary systems [21–26].

4. References

[1] Chalmers B 1961 *Physical Metallurgy* (New York: John Wiley)
[2] Laudise R A 1972 *The Growth of Single Crystals* (New York: Prentice Hall)
[3] Brice J S 1973 *The Growth of Crystals from Liquid* (Amsterdam: North Holland)
[4] Hobbs P V 1974 *Ice Physics* (Oxford: Clarendon)
[5] Alexandrov D V 2004 *Int. J. Heat Mass Trans.* **47** 1383–1389
[6] Herlach D M 2008 *Phase Transformations in Multicomponent Melts* (Weinheim: Wiley-VCH)
[7] Alexandrov D V and Malygin A P 2011 *Int. J. Heat Mass Trans.* **54** 1144–1149
[8] Alexandrov D V and Malygin A P 2012 *Int. J. Heat Mass Trans.* **55** 3196–3204
[9] Herlach D M 2015 *Crystals* **5** 355–375
[10] Alexandrova I V, Alexandrov D V, Aseev D L and Bulitcheva S V 2009 *Acta Physica Polonica A* **115** 791–794
[11] Hills R N, Loper D E and Roberts P H 1983 *Q. J. Appl. Math.* **36** 505–539
[12] Fowler A C 1985 *IMA J. Appl. Math.* **35** 159–174
[13] Borisov V T 1987 *Theory of Two-Phase Zone of Metallic Ingot* (Moscow: Metallurgia)
[14] Alexandrov D V 2001 *J. Crystal Growth* **222** 816–821
[15] Alexandrov D V, Nizovtseva I G, Malygin A P, Huang H-N and Lee D 2008 *J. Phys.: Condens. Matter* **20** 114105
[16] Alexandrov D V and Nizovtseva I G 2008 *Dokl. Earth Sci.* **419** 359–362
[17] Alexandrov D V, Ivanov A A and Malygin A P 2009 *Acta Physica Polonica A* **115** 795–799
[18] Alexandrov D V and Ivanov A A 2009 *Int. J. Heat Mass Trans.* **52** 4807–4811
[19] Huppert H E and Worster M G 1985 *Nature* **314** 703–707
[20] Worster M G 1986 *J. Fluid Mech.* **167** 481–501
[21] Alexandrov D V and Malygin A P 2013 *J. Phys. A: Math. Theor.* **46** 455101
[22] Alexandrov D V and Nizovtseva I G 2014 *Proc. R. Soc. A* **470** 20130647
[23] Alexandrov D V and Malygin A P 2014 *Modelling Simul. Mater. Sci. Eng.* **22** 015003
[24] Alexandrov D V 2014 *Phys. Lett. A* **378** 1501–1504
[25] Alexandrov D V 2014 *J. Phys. A: Math. Theor.* **47** 125102
[26] Alexandrov D V 2014 *Phil. Mag. Lett.* **94** 786–793

Acknowledgments

This work was supported by the Russian Science Foundation (grant no. 16-11-10095).